Cluster-Based Polarized Spectrum Sharing in Channels with Polarization Mode Dispersion

Dongming Li, Zhimin Zeng, Caili Guo, and Xiaolin Lin

Polarized spectrum sharing (PSS) exploits the spectrum opportunities in a polarized domain. However, when it comes to wideband environments PSS is impaired by the frequency-dependent polarization mode dispersion (PMD); thus, the effective throughput of PSS drops. To combat the PMD effect, this work proposes a cluster-based PSS approach to enable PSS on a narrower frequency span. Simulation results show that the effective throughput of PSS on cluster basis outperforms that of PSS on bandwidth and subcarrier basis.

Keywords: Polarization, spectrum opportunity, PMD, LTE.

I. Introduction

Polarization mode dispersion (PMD) is the polarization-sensitive frequency-selective fading effect of the channel in wideband environments; for example, the channel depolarization effects on different frequencies are distinct. In [1], it is shown that the output polarization states (PS) of the channel exhibit frequency-dependent dispersion if the channel has polarization-diverse multipath delay spreads.

Spectrum opportunities in the polarized domain are exploited for LTE user (LU) in [2]–[4], without considering the PMD effect. Polarized spectrum sharing (PSS) deployed on LTE operation bands suffers from adverse PMD effects. The performance of PSS drops, because undesired PS come into being on some frequency components after a unique PS transmits through the channel.

To avoid the PMD effect, this work proposes to enable PSS on a cluster of orthogonal frequency-division multiplexing (OFDM) subcarriers. As LU learns wideband environments before transmitting data, the subcarriers' number in the cluster impacts both the learning time and LU's throughput. Then, a learning-throughput tradeoff problem is formulated and solved.

II. System and Spectrum Opportunity Model

1. System and Channel Model

A coexistence scenario of primary users (PU) and LU is shown in Fig. 1. Dual polarized antennas on LU are used to derive arbitrary PS. LU's desired signal link is denoted by the matrix $\boldsymbol{H}_L$, interference links between PU and LU are denoted by $\boldsymbol{H}_{PL}$ and $\boldsymbol{H}_{LP}$, respectively, and $\boldsymbol{H}_m$ is the monitoring link used for learning environments by LU. Supposing that reciprocity [5] holds between $\boldsymbol{H}_{LP}$ and $\boldsymbol{H}_m$—namely, $\boldsymbol{H}_m = \boldsymbol{H}_{LP}^{\mathrm{H}}$, where superscript H denotes the Hermitian transpose. PU's PS is represented by $\boldsymbol{P}_c$, and the transmitting and receiving PS for LU are $\boldsymbol{P}_t$ and $\boldsymbol{P}_r$, respectively.

Due to the channel depolarization effect, some signal energy will be transferred from its original polarized component to its orthogonal one; thus, the signals' PS will be deflected. The channel matrix incorporating the depolarization effect [3] is

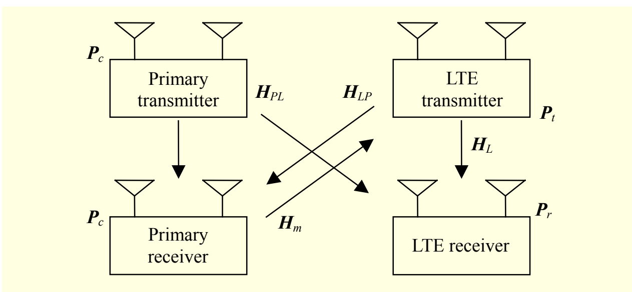

Fig. 1. Coexistence scenario of PU and LU.

Manuscript received Oct. 9, 2013; revised Dec. 7, 2013; accepted Dec. 30, 2013.

This work was supported by the Chinese National Nature Science Foundation (61271177), and the Fundamental Research Funds for the Central University (2013RC0108).

Dongming Li (phone: +86 18810535412, lidongming1986@gmail.com), Zhimin Zeng (zengzm@bupt.edu.cn), Caili Guo (guocaili@gmail.com), and Xiaolin Lin (linxiaolin1220@gmail.com) are with the School of Communication and Information Engineering, Beijing University of Posts and Telecommunications, Beijing, China.

http://dx.doi.org/10.4218/etrij.14.0213.0458

denoted as

$$\boldsymbol{H}_L = \begin{bmatrix} e^{j\alpha_1^L} & \sqrt{\mu_L \chi_L} e^{j\alpha_2^L} \\ \sqrt{\chi_L} e^{j\alpha_3^L} & \sqrt{\mu_L} e^{j\alpha_4^L} \end{bmatrix}, \tag{1}$$

where the co-polarization ratio $\mu_L \in [0,1]$ and the cross-polarization ratio $\chi_L \in [0,1]$ describe the power imbalance of the two orthogonal polarization components of the channel. The random phases of the polarization components α_i^L (i = 1, 2, 3, 4) are uniformly drawn over [0, 2π]. The channel matrices of $\boldsymbol{H}_{PL}$, $\boldsymbol{H}_{LP}$, and $\boldsymbol{H}_m$ can be similarly formulated.

2. Polarized Spectrum Opportunities

To avoid interfering PUs, the transmitting PS ($\boldsymbol{P}_t$) should be orthogonal to PU's receiving PS ($\boldsymbol{P}_c$) after transmitting through interference channel $\boldsymbol{H}_{SP}$; that is,

$$\boldsymbol{P}_c^{\mathrm{H}} \boldsymbol{H}_{LP} \boldsymbol{P}_t = (\boldsymbol{H}_{LP}^{\mathrm{H}} \boldsymbol{P}_c)^{\mathrm{H}} \boldsymbol{P}_t = 0. \tag{2}$$

Taking $\boldsymbol{H}_m$ = $\boldsymbol{H}_{LP}{}^{\mathrm{H}}$ into (2), we have $(\boldsymbol{H}_m \boldsymbol{P}_c)^{\mathrm{H}} \boldsymbol{P}_t = 0$. Defining $s_P(n)$ (n = 1, 2, …, N) as primary signals, where N is the number of samples, and equating both sides of $(\boldsymbol{H}_m \boldsymbol{P}_c)^{\mathrm{H}} \boldsymbol{P}_t = 0$ with $s_P(n)$ yields

$$[\boldsymbol{H}_m \boldsymbol{P}_c s_P(n)]^{\mathrm{H}} \boldsymbol{P}_t = 0. \tag{3}$$

Note that $\boldsymbol{H}_m \boldsymbol{P}_c s_P(n)$ is PU's signal received at LU; thus, based on (3), $\boldsymbol{P}_t$ can be derived by sampling PU's signals. The practically sampled PU's signals are represented as $\boldsymbol{Y}(n)$, which can be expressed as

$$\boldsymbol{Y}(n) = \boldsymbol{H}_m \boldsymbol{P}_c s_P(n) + \boldsymbol{\sigma}(n), \tag{4}$$

where the 2×1 vector $\boldsymbol{\sigma}(n)$ is additive noise; thus, the noise in $\boldsymbol{Y}(n)$ should be suppressed. The subspace-based noise suppression method has been studied in [3], where the noise-free primary signals can be obtained and defined as $\boldsymbol{V}(n) = \boldsymbol{H}_m \boldsymbol{P}_c s_P(n)$. Taking this equation into (4), we get

$$\frac{1}{N} \Sigma_{n=1}^{N} \boldsymbol{V}(n)^{\mathrm{H}} \boldsymbol{P}_t = 0. \tag{5}$$

Therefore, $\boldsymbol{P}_t$ can be derived according to (5).

Then, $\boldsymbol{P}_r$ should be designed to maximize LU's signal-to-interference-plus-noise-ratio (SINR). LU's received signal is

$$\boldsymbol{R} = \boldsymbol{P}_r^{\mathrm{H}} (\boldsymbol{H}_L \boldsymbol{P}_t s_L + \boldsymbol{H}_{PL} \boldsymbol{P}_c s_P) + \sigma_L, \tag{6}$$

where s_L and $\boldsymbol{\sigma}_L$ are LR's signal and noise, respectively. Then, the desired and interference signals' power are $\| \boldsymbol{P}_r^{\mathrm{H}} \boldsymbol{H}_L \boldsymbol{P}_t \|^2$ and $\| \boldsymbol{P}_r^{\mathrm{H}} \boldsymbol{H}_{PL} \boldsymbol{P}_c \|^2$, respectively; where $\| \cdot \|$ is the Euclidean norm. Thus LU's SINR should be maximized as

$$(\mathcal{P}_1) \ \underset{\boldsymbol{P}_r}{maximize} \frac{\| \boldsymbol{P}_r^{\mathrm{H}} \boldsymbol{H}_L \boldsymbol{P}_t \|^2}{\| \boldsymbol{P}_r^{\mathrm{H}} \boldsymbol{H}_{PL} \boldsymbol{P}_c \|^2 + \sigma_L^2}, \tag{7}$$

where σ_L^2 is the power of additive noise at LR. It is noteworthy that $\mathcal{P}_1$ is a generalized Rayleigh entropy problem, whose solution is well-known as

$$\boldsymbol{P}_r = \boldsymbol{v}_{\max}[(\boldsymbol{H}_{PL} \boldsymbol{P}_c \boldsymbol{P}_c^{\mathrm{H}} \boldsymbol{H}_{PL}^{\mathrm{H}} + \sigma_L^2 \mathbf{I}_2)^{-1} \boldsymbol{H}_L \boldsymbol{P}_t \boldsymbol{P}_t^{\mathrm{H}} \boldsymbol{H}_L^{\mathrm{H}}], \tag{8}$$

where $\mathbf{I}_2$ is an identity matrix of rank 2, $\boldsymbol{v}_{\max}[\cdot]$ is the eigenvector corresponding to the maximum eigenvalue, and $(\cdot)^{-1}$ is the inverse matrix.

III. Motivation

Suppose the bandwidth for LU is B, which starts from ω_0 and ends at ω_M, where M is the subcarrier number of the operation band. The channel depolarization effects are frequency-selective as a result of PMD. Thus $\boldsymbol{H}_L$, $\boldsymbol{H}_{PL}$, $\boldsymbol{H}_{LP}$, and $\boldsymbol{H}_m$ should be rewritten as $\boldsymbol{H}_L(\omega_i)$, $\boldsymbol{H}_{PL}(\omega_i)$, $\boldsymbol{H}_{LP}(\omega_i)$, and $\boldsymbol{H}_m(\omega_i)$, respectively.

In wideband environments, (2) should be rewritten as

$$\boldsymbol{P}_c^{\mathrm{H}} \boldsymbol{H}_{LP}(\omega_i) \boldsymbol{P}_t = [\boldsymbol{H}_{LP}^{\mathrm{H}}(\omega_i) \boldsymbol{P}_c]^{\mathrm{H}} \boldsymbol{P}_t = 0. \tag{9}$$

For $j \neq i$, $\boldsymbol{H}_{LP}(\omega_j) \neq \boldsymbol{H}_{LP}(\omega_i)$ holds due to PMD. Thus, if $\boldsymbol{H}_{LP}(\omega_i)\boldsymbol{P}_t$ satisfies (2), then $\boldsymbol{H}_{LP}(\omega_j) \boldsymbol{P}_t$ ($j \neq i$) will fail to satisfy (2), which means all the M-1 polarizations $\boldsymbol{H}_{LP}(\omega_j)\boldsymbol{P}_t$ ($j \in \{0, \cdots, M-1\}$ and $j \neq i$) from the LTE transmitter (LT) are not orthogonal with $\boldsymbol{P}_c$; thus, interference is inflicted on PU.

Similarly, due to the PMD effect, (7) should be rewritten as

$$\underset{\boldsymbol{P}_r}{maximize} \frac{\| \boldsymbol{P}_r^{\mathrm{H}} \boldsymbol{H}_L(\omega_i) \boldsymbol{P}_t \|^2}{\| \boldsymbol{P}_r^{\mathrm{H}} \boldsymbol{H}_{PL}(\omega_i) \boldsymbol{P}_c \|^2 + \sigma_L^2(\omega_i)}. \tag{10}$$

Both $\boldsymbol{H}_L(\omega_i)\boldsymbol{P}_t$ from LT in the numerator of (10) and $\boldsymbol{H}_{PL}(\omega_i)\boldsymbol{P}_c$ from PU in the denominator of (10) are desired for $\boldsymbol{P}_r$ at LR. Then, $\boldsymbol{H}_L(\omega_j)\boldsymbol{P}_t$ ($j \neq i$) and $\boldsymbol{H}_{PL}(\omega_j)\boldsymbol{P}_t$ ($j \neq i$) are undesired for $\boldsymbol{P}_r$; thus, LTE throughput performance drops.

IV. Cluster-Based PSS

To combat the PMD effect, the frequency span for $\boldsymbol{P}_t$ and $\boldsymbol{P}_r$ is reduced from B to a cluster of several subcarriers, as shown in Fig. 2. For descriptive convenience, the channels' subscripts are omitted and the channel matrices are simplified as $\boldsymbol{H}(\omega_i)$. The number of subcarriers in each cluster is denoted as X. Then, the number of clusters on the entire operation band is $\left\lfloor \frac{M}{X} \right\rfloor + 1$, where $\lfloor \cdot \rfloor$ represents the floor function. There are $M - X\left\lfloor \frac{M}{X} \right\rfloor$

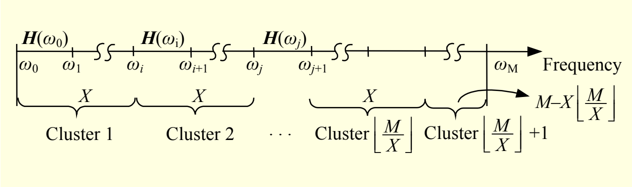

Fig. 2. Cluster-based LTE operation band.

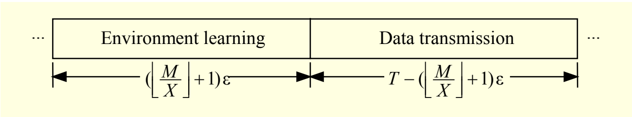

Fig. 3. Two-phase frame for PSS.

subcarriers in the $(\left\lfloor \frac{M}{X} \right\rfloor + 1)$th cluster.

An LTE frame usually contains environment learning and data transmission phases. As shown in Fig. 3, the frame length is T. The learning time for each cluster with N samples is ε, then the overall learning time for all clusters is $(\left\lfloor \frac{M}{X} \right\rfloor + 1)\varepsilon$. The remaining time $T-(\left\lfloor \frac{M}{X} \right\rfloor + 1)\varepsilon$, is used to transmit data.

For cluster-based PSS, the transmitting or receiving polarization for all subcarriers inside a cluster is unique—for example, the transmitting and receiving polarizations for jth cluster are respectively $\boldsymbol{P}_t^j$ and $\boldsymbol{P}_r^j$. Moreover, for ith subcarrier in jth cluster, $\boldsymbol{H}_{PL}(\omega)$, $\boldsymbol{H}_{LP}(\omega)$, $\boldsymbol{H}_L(\omega)$, and $\boldsymbol{H}_m(\omega)$ should be further rewritten as $\boldsymbol{H}_{PL}(i, j)$, $\boldsymbol{H}_{LP}(i, j)$, $\boldsymbol{H}_L(i, j)$, and $\boldsymbol{H}_m(i, j)$, respectively.

Thus, the effective LTE throughput can be formulated as

$$\gamma(X) = \frac{T-\left(\left\lfloor \frac{M}{X} \right\rfloor + 1\right)\varepsilon}{T} \log_2\left[1+\frac{S(X)}{I(X)+\Sigma_{i=1}^{M}\sigma_{L,i}^2}\right], \quad (11)$$

where $\sigma_{L,i}^2$ is the noise power on ith subcarrier, and

$$S(X) = \Sigma_{j=1}^{\left\lfloor \frac{M}{X} \right\rfloor}\Sigma_{i=1}^{X} \| (\boldsymbol{P}_r^j)^{\mathrm{H}} \boldsymbol{H}_L(i,j)\boldsymbol{P}_t^j \|^2 + \Sigma_{i=1}^{M-X\left\lfloor \frac{M}{X} \right\rfloor} \| (\boldsymbol{P}_r^{\left\lfloor \frac{M}{X} \right\rfloor+1})^{\mathrm{H}} \boldsymbol{H}_L(i, \left\lfloor \frac{M}{X} \right\rfloor + 1)\boldsymbol{P}_t^{\left\lfloor \frac{M}{X} \right\rfloor+1} \|^2,$$

$$I(X) = \Sigma_{j=1}^{\left\lfloor \frac{M}{X} \right\rfloor}\Sigma_{i=1}^{X} \| (\boldsymbol{P}_r^j)^{\mathrm{H}} \boldsymbol{H}_{PL}(i,j)\boldsymbol{P}_c \|^2 + \Sigma_{i=1}^{M-X\left\lfloor \frac{M}{X} \right\rfloor} \| (\boldsymbol{P}_r^{\left\lfloor \frac{M}{X} \right\rfloor+1})^{\mathrm{H}} \boldsymbol{H}_{PL}(i, \left\lfloor \frac{M}{X} \right\rfloor + 1)\boldsymbol{P}_c \|^2. \quad (12)$$

Since X represents the frequency span for PSS, it can be noted from (11) that a smaller X is desirable for learning a wideband environment more precisely and further minimizing the PMD effect. However, a larger X is desirable for achieving a smaller $(\left\lfloor \frac{M}{X} \right\rfloor + 1)\varepsilon$ and more time for data transmission.

Particularly, when X=1, the primary signals are sampled on each subcarrier to learn the environment. This case is termed as subcarrier-based PSS. Although the environment is learned more precisely and a slight PMD effect exists, more time is used for learning environment and less time is used for transmitting data. When X=M, the primary signals are sampled on the entire operation band. This case is termed as band-based PSS. Although the environment is learned less precisely and a severe PMD effect exists, more time is used for data transmission.

Therefore, different choices of X lead to different tradeoffs between environment learning and throughput maximization. With the interference to PUs taken into consideration, the learning-throughput tradeoff problem can be formulated as

$$(\mathcal{P}_2) \quad \underset{X}{maximize}\ \gamma(X), \quad \text{subject to}\ \ \zeta(X) \le \delta, \quad (13)$$

where $\zeta(X)$ is the interference inflicted on PU, and δ is the tolerable interference power. The interference $\zeta(X)$ is formulated as

$$\zeta(X) = \Sigma_{j=1}^{\left\lfloor \frac{M}{X} \right\rfloor}\Sigma_{i=1}^{X} \| \boldsymbol{P}_c^{\mathrm{H}} \boldsymbol{H}_{LP}(i,j)\boldsymbol{P}_t^j \|^2 + \Sigma_{i=1}^{M-X\left\lfloor \frac{M}{X} \right\rfloor} \| \boldsymbol{P}_c^{\mathrm{H}} \boldsymbol{H}_{LP}(i, \left\lfloor \frac{M}{X} \right\rfloor + 1)\boldsymbol{P}_t^{\left\lfloor \frac{M}{X} \right\rfloor+1} \|^2. \quad (14)$$

Since the value of X is discrete, $\gamma(X)$ and $\zeta(X)$ are non-differentiable and the convexity of $\mathcal{P}_2$ cannot be determined. Thus it is impossible to analytically derive the optimal solutions of $\mathcal{P}_2$. Genetic algorithms (GA) [7] are used to get the optimal solutions, as shown in Algorithm 1.

Algorithm 1 Genetic searching of optimal X.

1. (Initialization): Randomly initiate X as X_0, calculate $\gamma(X_0)$ and $\zeta(X_0)$ according to (11) and (14). If $\zeta(X_0) > \delta$, discard X_0 and repeat step 1.
2. (Evolution): Generate the evolutionary subcarrier number X_e according to the evolutionary operation defined by GA. Calculate $\gamma(X_e)$ and $\zeta(X_e)$. If $\zeta(X_e) > \delta$, discard X_e and repeat step 2.
3. (Comparison and selection): The optimal subcarrier number in past iterations is denoted as X_{opt}. Compare $\gamma(X_{opt})$ and $\zeta(X_{opt})$, select the subcarrier number that generates greater effective throughput.
4. Check the termination condition, decide go to step 2 or terminate.

V. Simulation Results

In this section, the performance of the cluster-based PSS is validated by simulations. According to LTE specifications, M can be set as 72, 180, 300, 600, 900, or 1,200, and T is set as 10 ms. The time overhead of environment learning with N samples, (ε) is set as 0.5 ms [8]. The length of OFDM

http://dx.doi.org/10.4218/etrij.14.0213.0458

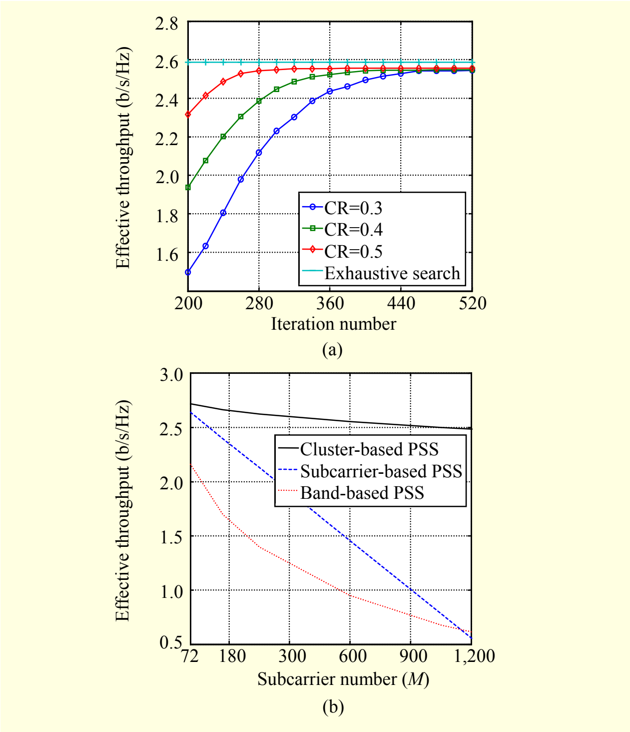

Fig. 4. Simulation results: (a) convergence performance of DE and (b) effective throughput for each mode of PSS.

subcarriers is set as 64, and the length of the cyclic prefix is 16. The transmit power of LU is fixed at 49 dBm [6]. Quadrature phase-shift keying is adopted as the modulation scheme. Differential evolution (DE) [7] is used to solve $\mathcal{P}_2$, and the cross-over (CR) factor is a key parameter for the convergence performance of DE. Greater values of CR$\in$[0, 1] will lead to a more rapid convergence; the empirical value of CR varies between 0.3 and 0.5 [7]. PU's receiveing PS ($\boldsymbol{P}_c$) is set as horizontal polarized. Parameters μ_L, χ_L and α_i^L are initiated randomly [8]; the results of over one million simulations are averaged to remove randomness.

Firstly, the convergence performance of DE for solving $\mathcal{P}_2$ is given in Fig. 4(a). For comparison, exhaustive search with step size ΔX=1 is used as the upper bound of achievable effective throughput. It can be noted that the effective throughput increases with the iteration number and converges gradually. Greater values of CR enable DE converge more rapidly. It can be also noted that the performance gap between exhaustive search and DE is minor after DE converges; thus, DE can efficiently converge to the optimal effective throughput.

The effective throughput for each mode of PSS is shown in Fig. 4(b). It can be noted that cluster-based PSS outperforms subcarrier-based and band-based PSS. The reason is that subcarrier-based PSS decreases the time for data transmission, while the band-based PSS deteriorates the achievable SINR, because of PMD. Cluster-based PSS outperforms, because it balances between subcarrier-based and band-based PSS.

It can also be noted from Fig. 4(b) that the performance improvements of cluster-based PSS over subcarrier-based and band-based PSS increase with the bandwidth. Since greater bandwidth will exhibit more severe PMD effects, cluster-based PSS gains more effective throughput improvements.

Moreover, the effective throughput for each mode of PSS decreases with M. As subcarrier-based PSS is free of PMD effect, the achievable SINR remains constant, but the data transmission time decreases linearly with M. For band-based PSS, the data transmission time holds constant but is impaired by the PMD effect. As the PMD effect; accumulates with M, the effective throughput decreases with M. Cluster-based PSS balances the data transmission time and PMD effect; thus, its effective throughput decreases more slightly with M.

VI. Conclusion

Wideband polarization spectrum sharing is studied for LTE in this work. By deploying PSS on a cluster of OFDM subcarriers, not only adverse PMD effects can be suppressed, but also the time used for data transmission can be increased; thus, the effective throughput performance is improved.

References

[1] T. Pratt, B. Walkenhorst, and S. Nguyen, "Adaptive Polarization Transmission of OFDM Signals in Channels with Polarization Mode Dispersion and Polarization-Dependent Loss," *IEEE Trans. Wireless Commun.*, vol. 8, no. 7, July 2009, pp. 3354–3359.

[2] D. Li et al., "A Novel Underlay TV Spectrum Sharing Scheme Based on Polarization Adaption for TD-LTE System," *Proc. IEEE WCNC*, Shanghai, China, Apr. 7–10, 2013, pp. 2484–2489.

[3] X. Lin et al., "A Novel Interference Avoidance Scheme Based on Blind Polarization Signal Processing for Cognitive Femtocell Network," *Proc. Int. Symp. WPMC*, Taiwan, Sept. 2012, pp. 40–44.

[4] B. Cao et al., "Exploiting Orthogonally Dual-Polarized Antennas in Cooperative Cognitive Radio Networking," *J. IEEE Sel. Areas Commun.*, vol. 31, no. 11, Nov. 2013, pp. 2362–2373.

[5] S. Haile, *Investigation of Channel Reciprocity for OFDM TDD Systems*, MS Thesis, Dept. Electr. Eng., UW., Canada, 2009.

[6] Y.-C. Liang et al., "Sensing-Throughput Tradeoff for Cognitive Radio Networks," *IEEE Trans. Wireless Commun.*, vol. 7, no. 4, Apr. 2008, pp. 1326–1337.

[7] S.M. Elsayed et al., "An improved Self-Adaptive Differential Evoulution Algorithm for Optimization Problems," *IEEE Trans. Ind. Informat.*, vol. 9, no. 1, Feb. 2013, pp. 89–99.

[8] C. Oestges and B. Clerckx, *MIMO Wireless Communications: From Real-World Propagation to Space-Time Code Design*, 1st ed., Oxford, UK: Elsevier-Academic Press, 2007.